



### 저작자표시-비영리-변경금지 2.0 대한민국

이용자는 아래의 조건을 따르는 경우에 한하여 자유롭게

- 이 저작물을 복제, 배포, 전송, 전시, 공연 및 방송할 수 있습니다.

다음과 같은 조건을 따라야 합니다:



저작자표시. 귀하는 원 저작자를 표시하여야 합니다.



비영리. 귀하는 이 저작물을 영리 목적으로 이용할 수 없습니다.



변경금지. 귀하는 이 저작물을 개작, 변형 또는 가공할 수 없습니다.

- 귀하는, 이 저작물의 재이용이나 배포의 경우, 이 저작물에 적용된 이용허락조건을 명확하게 나타내어야 합니다.
- 저작권자로부터 별도의 허가를 받으면 이러한 조건들은 적용되지 않습니다.

저작권법에 따른 이용자의 권리와 책임은 위의 내용에 의하여 영향을 받지 않습니다.

이것은 [이용허락규약\(Legal Code\)](#)을 이해하기 쉽게 요약한 것입니다.

[Disclaimer](#)



의학박사 학위논문

A population pharmacokinetic  
study of fludarabine in  
paediatric patients undergoing  
haematopoietic stem cell  
transplantation

소아 조혈모세포이식 환자에서  
플루다라빈의 집단약동학 연구

2018년 08월

서울대학교 대학원  
의과학과 의과학전공  
정 혜 원

A thesis of the Degree of Doctor of Philosophy

소아 조혈모세포이식 환자에서  
플루다라빈의 집단약동학 연구

A population pharmacokinetic  
study of fludarabine in  
paediatric patients undergoing  
haematopoietic stem cell  
transplantation

August 2018

The Department of Biomedical Sciences,  
Seoul National University  
College of Medicine  
Hyewon Chung

## ABSTRACT

**Introduction:** Fludarabine is used as a common component of conditioning regimens for haematopoietic stem cell transplantation (HSCT). However, knowledge regarding the pharmacokinetic characteristics of once-daily fludarabine dosing in children is limited. This study investigated the pharmacokinetics of fludarabine and explored its associations with clinical outcomes in paediatric patients.

**Methods:** A total of 802 concentration data obtained from 43 paediatric patients who underwent HSCT and administered fludarabine were included in a population pharmacokinetic analysis using non-linear mixed-effects modelling. Based on individual systemic exposures derived from the model, associations between F-ara-A exposure and clinical outcome variables were explored.

**Results:** A two-compartment model with proportional residual

error adequately described the concentration–time profile of F–ara–A. The body surface area (BSA) and glomerular filtration rate were significant covariates for the clearance of F–ara–A. No significant associations were found between systemic exposure and graft–versus–host disease, relapse or survival.

**Conclusion:** This study evaluated the pharmacokinetics of F–ara–A after fludarabine administration in paediatric patients. Comparable systemic exposure to that of previous reports from adults may support the appropriateness of BSA–based dosing in children.

\* Part of this work has been published in Bone Marrow Transplantation (Chung H, et al. Bone Marrow Transplant. 2018 Jun 18. doi: 10.1038/s41409–018–0260–z).

---

**Keywords:** Pharmacokinetics, Modelling, Paediatric, Fludarabine

**Student number:** 2013–21790

# CONTENTS

ABSTRACT .....	i
CONTENTS .....	iii
LIST OF TABLES .....	v
LIST OF FIGURES .....	vi
LIST OF ABBREVIATIONS .....	viii
INTRODUCTION .....	1
METHODS .....	5
Study population and study design .....	5
Population pharmacokinetic analysis .....	6
Model validation .....	9
Statistical analysis .....	10
RESULTS .....	11
Characteristics of the patients and fludarabine administration .....	11

Pharmacokinetics .....	16
Exposure-clinical outcome relationships .....	29
DISCUSSION .....	39
REFERENCES .....	45
APPENDICES .....	55
1. Individual fitting plots.....	55
2. NONMEM control for the final model.....	58
국문 초록 .....	61

## LIST OF TABLES

Table 1. Patient demographics.....	12
Table 2. Summary of conditioning regimens.....	14
Table 3. Parameter estimates of the final model and bootstrap analysis results. ....	17
Table 4. Pharmacokinetic parameters of 9- $\beta$ -D-arabinofuranosyl-2-fluoroadenine (F-ara-A) after the first dose of fludarabine at 40 mg/m <sup>2</sup> . ....	27
Table 5. Incidence of complications after fludarabine administration according to 9- $\beta$ -D-arabinofuranosyl-2-fluoroadenine (F-ara-A) exposure using median value as a cut-off. ....	33
Table 6. Incidence of complications after fludarabine administration according to 9- $\beta$ -D-arabinofuranosyl-2-fluoroadenine (F-ara-A) exposure using 36,000 ng · h/mL as a cut-off.....	37

# LIST OF FIGURES

Figure 1. Goodness-of-fit plots for the plasma 9- $\beta$ -D-arabinofuranosyl-2-fluoroadenine (F-ara-A) concentration.....	21
Figure 2. Visual predictive check of the plasma concentration-time profiles of 9- $\beta$ -D-arabinofuranosyl-2-fluoroadenine (F-ara-A) using the final model.....	22
Figure 3. Visual predictive check comparing the observed plasma concentration-time profiles of 9- $\beta$ -D-arabinofuranosyl-2-fluoroadenine (F-ara-A) to the simulated data from previously published pharmacokinetic model. ....	23
Figure 4. Number of patients according to the cumulative area under the concentration-time curve ( $AUC_{cum}$ ) of 9- $\beta$ -D-arabinofuranosyl-2-fluoroadenine (F-ara-A).....	25
Figure 5. Number of patients according to the area under the concentration-time curve from dosing to 24 h post-dosing ( $AUC_{0-24}$ ) of 9- $\beta$ -D-arabinofuranosyl-2-fluoroadenine (F-ara-A) after the first dose of 40 mg/m <sup>2</sup> . ....	26

Figure 6. Relationships between the cumulative area under the curve (AUC) of 9- $\beta$ -D-arabinofuranosyl-2-fluoroadenine (F-ara-A) and the clinical outcomes.....	32
Figure 7. (a) Overall survival and (b) event-free survival according to cumulative area under the concentration-time curve (AUC <sub>cum</sub> ) of 9- $\beta$ -D-arabinofuranosyl-2-fluoroadenine (F-ara-A) using median value as a cut-off. ....	34
Figure 8. Relationships between the maximum concentration of 9- $\beta$ -D-arabinofuranosyl-2-fluoroadenine (F-ara-A) and the clinical outcomes.....	36
Figure 9. (a) Overall survival and (b) event-free survival according to cumulative area under the concentration-time curve (AUC <sub>cum</sub> ) of 9- $\beta$ -D-arabinofuranosyl-2-fluoroadenine (F-ara-A) using 36,000 ng·h/mL as a cut-off. ....	38

## LIST OF ABBREVIATIONS

AUC	area under the concentration–time curve
AUC <sub>0–24</sub>	AUC from dosing to 24 h post–dosing
AUC <sub>cum</sub>	cumulative AUC
AUC <sub>inf</sub>	AUC from dosing to infinity
BSA	body surface area
CI	confidence interval
CL	clearance
C <sub>max</sub>	maximum concentration
CWRES	conditional weighted residuals
EFS	event–free survival
F–ara–A	9– $\beta$ –D–arabinofuranosyl–2–fluoroadenine
F–ara–ATP	fludarabine triphosphate
GFR	glomerular filtration rate
GVHD	graft–versus–host disease
aGVHD	acute GVHD
cGVHD	chronic GVHD
HSCT	haematopoietic stem cell transplantation

NRM	non-relapse mortality
OFV	objective function value
OS	overall survival
PK	pharmacokinetic
Q	inter-compartmental clearance
RSE	relative standard error
$t_{1/2}$	terminal elimination half-life
TRM	treatment-related mortality
V1	central volume of distribution
V2	peripheral volume of distribution
VOD	veno-occlusive disease

# INTRODUCTION

Anatomical and physiological differences between paediatric and adult populations may lead to differential drug absorption, distribution, metabolism and excretion, which can consequently influence the drug response or effectiveness (1). Therefore, appropriate information based on paediatric clinical studies is needed to ensure the safe use of drugs in this population. For newly developed drugs, such studies are now required or encouraged with incentives such as additional exclusivity or patent protection by regulatory agencies.

However, numerous drugs were approved before the imposition of the regulations and one of these drugs is fludarabine, which has become an essential component in many reduced-intensity or non-myeloablative haematopoietic stem cell transplantation (HSCT) conditioning regimens. These regimens have shown clinical outcomes in adults with haematological malignancies that are comparable or superior to those of other regimens (2–6). Decreased treatment-related mortality (TRM) and possible graft-versus-leukaemia effects

contribute to these promising results (6). Nevertheless, the data are insufficient to establish the efficacy of fludarabine in any childhood malignancy (7). Consequently, the drug remains unapproved for paediatric use, although conditioning regimens with fludarabine are preferred for haematological malignancies (8, 9), severe aplastic anaemia and other rare genetic diseases in children (10, 11).

Fludarabine, which has potent immunosuppressive and anti-leukaemic properties, is a purine analogue whose principal action is inhibition of DNA synthesis. After administration, this drug is rapidly dephosphorylated in plasma to  $9-\beta$ -D-arabinofuranosyl-2-fluoroadenine (F-ara-A), which is taken up into cells and phosphorylated into fludarabine triphosphate (F-ara-ATP) (12). F-ara-ATP is the active form of the drug, which competes with deoxyadenosine 5'-triphosphate for incorporation into the growing DNA strands (13). Although studied in leukaemic cells, the results of F-ara-ATP concentration-dependent inhibition of DNA synthesis as well as a linear relationship between F-ara-A exposure and the F-ara-ATP level support that the pharmacokinetics of F-ara-A may

be predictive of the clinical outcomes of fludarabine treatment (14, 15).

Efforts have been made to explore the pharmacokinetics, pharmacodynamics, and their relationships with fludarabine in HSCT settings. However, the associations remain controversial, probably because of the variable study conditions such as conditioning regimens, disease status at transplantation, and diagnosis. Some researchers have reported associations between pharmacokinetic (PK) parameters and clinical outcomes such as overall survival (OS) or non-relapse mortality (NRM) and have suggested personalized dosing of fludarabine (16, 17). In contrast, other studies showed no association between PK parameters and clinical outcomes (2, 18, 19). Studies that used F-ara-A exposure and intracellular accumulation of F-ara-ATP in CD4+ and CD8+ cells as pharmacological biomarkers also showed no significant association with clinical outcomes (20, 21). A recent study in paediatric patients showed no association between exposure and TRM (22).

In paediatric patients, the pharmacokinetics of fludarabine are poorly understood due to the limited studies regarding

fludarabine (23). Two studies in paediatric patients with leukaemia and solid tumours have examined the pharmacokinetics of fludarabine, however, fludarabine was administered in bolus and continuous infusions and the dose administered was lower than that used in HSCT (24, 25). Currently, there is only one recent publication which reported data from paediatric patients undergoing HSCT after once-daily dosing with fludarabine (22). Moreover, no fludarabine PK data are available for Asian patients regardless of age. Therefore, the aim of the study was to build a population PK model of F-ara-A and to investigate the PK characteristics in paediatric patients undergoing allogeneic HSCT. In addition, the associations between clinical outcomes and systemic exposure of fludarabine were explored.

## METHODS

### Study population and study design

The plasma concentration of F-ara-A and clinical outcome data were obtained from a single-centre, prospective study. The study enrolled a total of 43 Korean patients who underwent HSCT at Seoul National University Children's Hospital between November 2011 and April 2014. Patients who received a fludarabine-conditioning regimen, were less than 19 years old, had an Eastern Cooperative Oncology Group performance status of 0–2, were free of significant functional problems in major organs and did not have any active viral or fungal infections were included. This study was approved by the Institutional Review Board of Seoul National University Hospital (H-1107-055-369) and was registered at [www.clinicaltrials.gov](http://www.clinicaltrials.gov) (NCT01472055). All patients provided written informed consent prior to the study procedure.

The intravenous fludarabine dose was based on the body surface area (BSA) calculated using the patient's actual body weight. For those who administered busulfan, 120 mg/m<sup>2</sup> was

administered once daily as the first dose on day -8, and then a dose was used from days -7 to -5 according to the therapeutic drug monitoring results to target a cumulative exposure of 75,000  $\mu\text{g}\cdot\text{h}/\text{L}$  (26, 27).

Initially, blood samples were collected at pre-dosing and at 0.5, 1, 3, 5, and 8 h post-dosing for 6 days. After an interim analysis with 6 patients found that a steady state was achieved from the second day of dosing, the time points for blood sampling were reduced to every pre-dose of fludarabine and at 0.5, 1, 3, 5, and 8 h post-dosing on the first and last days of dosing. Toxicity data were collected from the first administration of fludarabine until 180 days after HSCT.

## Population pharmacokinetic analysis

A total of 802 samples from 43 patients were used for the population PK analysis. The analysis was performed using non-linear mixed-effects modelling as implemented in NONMEM (version 7.3, ICON Development Solutions, Ellicott City, MD, USA). The first order conditional estimation with interaction

method was used. Because the measured F-ara-A was different from fludarabine phosphate (the administered form), a dose of F-ara-A (molecular weight: 285 g/mol) equivalent to the dose of fludarabine phosphate (365 g/mol) was used for modelling.

Inter-individual variability was modelled exponentially to each PK parameter as shown below:

$$P_{ij} = \theta_j \cdot \exp(\eta_{ij}) \quad (\text{Eq. 1})$$

, where  $P_{ij}$  is the  $j$ -th PK parameter for  $i$ -th individual,  $\theta_j$  is the typical value for the  $j$ -th parameter, and  $\eta_{ij}$  is a random variable assumed to be normally distributed with mean of 0 and a variance of  $\omega^2$ . The residual variability was evaluated using combined additive and proportional error model.

Candidate covariates, such as the BSA, weight, age, serum creatinine level, glomerular filtration rate (GFR) and sex were explored. The GFR was obtained using the method of Broechner-Mortensen and Roedbro (28, 29).

Model selection was based on decreases in the objective function value (OFV) and visual inspection of diagnostic plots. Scatter plot for all covariates were also plotted to assess the co-

linearity among the covariates. Continuous variables were added into the model using power functions:

$$\theta_j = \theta_n \times \left( \frac{Var_k}{Median\ value} \right)^{\theta_m} \quad (Eq.\ 2)$$

, where  $\theta_n$  is the population parameter estimate not explained by any of the covariates,  $Var_k$  is the  $k$ -th continuous variable and it is centered to the median value, and  $\theta_m$  is the exponent of the power function. Each covariate was added one at a time for forward selection. Decrease in OFV by 3.84 after adding a single covariate was identified as significant ( $P < 0.05$ ). For backward elimination, increase in OFV at least 6.63 when a covariate was deleted from the full model was used as a significant criteria ( $P < 0.01$ ) to retain the covariate in the model.

Based on the final model, individual concentrations were predicted every 15 minutes from the time of the first infusion to 24 h after the last infusion of fludarabine. Daily values of the maximum concentration ( $C_{max}$ ), terminal elimination half-life ( $t_{1/2}$ ), area under the concentration-time curve (AUC) from dosing to 24 h post-dosing ( $AUC_{0-24}$ ), and AUC from dosing to infinity ( $AUC_{inf}$ ) were derived from the individual predicted concentrations using a non-compartmental method using

Phoenix® WinNonlin® (Version 7.0.0., Certara, Princeton, NJ, USA). The cumulative AUC ( $AUC_{cum}$ ) was calculated as the sum of the  $AUC_{0-24}$  values from 5 or 6 days of dosing. The accumulation ratio was calculated as the  $AUC_{0-24}$  on the last day of dosing divided by the  $AUC_{0-24}$  on the first day of dosing.

## Model validation

Model validation was conducted by performing a visual predictive check with 1,000 simulations. The 95% confidence intervals (CIs) for the 5<sup>th</sup>, 50<sup>th</sup> and 95<sup>th</sup> predicted percentiles were visually compared with the observed data. The visual predictive check was also used to compare our data with simulated data based on the PK model and parameter estimates reported in a previous publication (30). In addition, a nonparametric bootstrap was performed to evaluate the stability and robustness of the model. The final model was fitted repeatedly to 1,000 resampled datasets. The medians of the PK parameters were obtained and 2.5<sup>th</sup> and 97.5<sup>th</sup> percentiles were regarded as the lower and upper limits of 95% CI. The values were compared with the parameter

estimates from the final model.

## Statistical analysis

The categorical and continuous variables were compared using the Fisher's exact test and the Mann–Whitney U test, respectively. The incidence rates of relapse, NRM, acute graft–versus–host disease (aGVHD) and chronic GVHD (cGVHD) were calculated using a cumulative incidence function. OS and event–free survival (EFS) were analysed using the Kaplan–Meier method. Differences in the cumulative incidence curves were examined using Gray's test, whereas differences in the survival rates were determined using the log–rank test. The statistical analyses were performed using ‘R’ version 3.2.2 ([www.r-project.org](http://www.r-project.org)) and SAS 9.4 (SAS Institute Inc., Cary, NC, USA). Statistical significance was accepted when  $P < 0.05$ .

## RESULTS

### Characteristics of the patients and fludarabine administration

The clinical characteristics of the patients included in the population PK analysis are summarized in Table 1. Among the 43 patients enrolled, 31 were males and 12 were females with ages ranging from 1.3 to 18.5 years. Forty-three patients underwent HSCT using a fludarabine-containing conditioning regimen (Table 2). Forty patients received a six-day fludarabine regimen. Of these patients, the dosage of fludarabine was  $40 \text{ mg/m}^2/\text{day}$  in 37 patients and  $40 \text{ mg/m}^2/\text{day}$  for 5 days and  $30 \text{ mg/m}^2/\text{day}$  for the last day in one patient due to azotaemia. In the remaining 2 patients, the dosage was reduced to  $30 \text{ mg/m}^2/\text{day}$  and  $34 \text{ mg/m}^2/\text{day}$  due to impaired renal function with a low GFR of  $60.9 \text{ mL/min}/1.73 \text{ m}^2$  and a low body weight of 9.5 kg, respectively. Three patients received a five-day fludarabine regimen with a daily dose of  $40 \text{ mg/m}^2$  due to different conditioning regimen schedules.

**Table 1. Patient demographics.**

Characteristics	n = 43
Median age, year (range)	11.8 (1.3–18.5)
Body weight, kg (range)	39.9 (9.5–76.2)
Body surface area, m <sup>2</sup> (range)	1.3 (0.4–1.9)
Glomerular filtration rate, mL/min/1.73 m <sup>2</sup>	132.6 (60.9–299.2)
Gender, No. (%)	
Male	31 (72.1)
Female	12 (27.9)
Diagnosis, No. (%)	
Acute leukaemia	29 (67.4)
Other malignancies <sup>a</sup>	2 (4.7)
Severe aplastic anaemia	3 (7.0)
Chronic granulomatous disease	3 (7.0)
Osteopetrosis	2 (4.7)
Others <sup>b</sup>	4 (9.3)
Cumulative busulfan exposure, μg·h/L	74,706 (70,996 – 79,862)

---

Characteristics	n = 43
<b>Stem cell source</b>	
Peripheral blood	31 (72.1)
Bone marrow	8 (18.6)
Cord blood	4 (9.3)
<b>Donor type</b>	
Related	6 (14.0)
Unrelated	34 (79.1)
Haploidentical	3 (7.0)

---

No. indicates number.

<sup>a</sup> 1 juvenile myelomonocytic leukaemia and 1 anaplastic large cell lymphoma

<sup>b</sup> 1 Haemophagocytic lymphohistiocytosis, 1 Wiskott–Aldrich syndrome, 1 Adrenoleukodystrophy and 1 Krabbe disease.

**Table 2. Summary of conditioning regimens.**

Regimen	Number of patients	Fludarabine dosage	Other conditioning regimen
BuFluVP	23	40 mg/m <sup>2</sup> /day for 6 days  (days -8 to -3)	Targeted busulfan  Etoposide 20 mg/kg/day i.v. on days -4 to -2  ATG 2.5 mg/kg/day i.v. on days -4 to -2
	1	30 mg/m <sup>2</sup> /day for 6 days  (days -8 to -3)	Targeted busulfan  Etoposide 20 mg/kg/day i.v. on days -4 to -2  ATG 2.5 mg/kg/day i.v. on days -4 to -2
BuFlu	11	40 mg/m <sup>2</sup> /day for 6 days  (days -8 to -3)	Targeted busulfan  ATG 2.5 mg/kg/day i.v. on days -4 to -2
	1	34 mg/m <sup>2</sup> /day for 6 days  (days -8 to -3)	Targeted busulfan  ATG 2.5 mg/kg/day i.v. on days -4 to -2

Regimen	Number of patients	Fludarabine dosage	Other conditioning regimen
BuFluMel	3	40 mg/m <sup>2</sup> /day for 6 days (days -8 to -3)	Targeted busulfan Melphalan 70mg/m <sup>2</sup> /day i.v. on days 3- and -2 ATG 2.5 mg/kg/day i.v. on days -4 to -2
	1	40 mg/m <sup>2</sup> /day for 5 days (days -8 to -4) and 30 mg/m <sup>2</sup> /day for 1 day (day -3)	Targeted busulfan Melphalan 70mg/m <sup>2</sup> /day i.v. on days 3- and -3 ATG 2.5 mg/kg/day i.v. on days -4 to -2
CyFlu	2	40 mg/m <sup>2</sup> /day for 5 days (days -6 to -2)	Cyclophosphamide 60 mg/kg/day i.v. on days -8 and -7 ATG 2.5 mg/kg/day i.v. on days -4 to -2
BuFluCy	1	40 mg/m <sup>2</sup> /day for 5 days (days -8 to -4)	Targeted busulfan Cyclophosphamide 14.5 mg/kg/day i.v. on days -3 and -2

Bu, busulfan; Flu, fludarabine; VP, etoposide; Mel, melphalan; Cy, cyclophosphamide; ATG, Anti-thymoglobulin.

## Pharmacokinetics

A two-compartment model with first-order elimination and proportional residual error adequately described the pharmacokinetics of F-ara-A. The clearance (CL), central volume of distribution (V1), peripheral volume of distribution (V2) and inter-compartmental clearance (Q) were estimated from the model. The selected final model included exponential random effects for inter-individual variability on CL, V1, V2, and Q. A variance-covariance block matrix was applied among CL, V1 and V2. BSA was a significant covariate for CL, V1 and V2 using a power function, whereas the GFR was significant for CL. The typical population estimates of CL, V1, V2 and Q for a subject with a BSA of 1.254 m<sup>2</sup> and a GFR of 132.6 mL/min/1.73 m<sup>2</sup> were 8.08 L/h, 28.8 L, 33.8 L and 5.81 L/h, respectively (Table 3).

Table 3. Parameter estimates of the final model and bootstrap analysis results.

Parameter	Estimate	RSE (%)	Bootstrap median	Bootstrap 95% CI
$CL \text{ (L/h)} = \theta_{CL} \cdot (BSA/1.254)^{\theta_{BSA \text{ on } CL}} \cdot (GFR/132.6)^{\theta_{GFR \text{ on } CL}}$				
$\theta_{CL}$	8.08	4.1	8.1	[7.48 – 8.73]
$\theta_{BSA \text{ on } CL}$	0.966	11.8	0.974	[0.746 – 1.24]
$\theta_{GFR \text{ on } CL}$	0.493	21.7	0.496	[0.246 – 0.727]
$V1 \text{ (L)} = \theta_{V1} \cdot (BSA/1.254)^{\theta_{BSA \text{ on } V1}}$				
$\theta_{V1}$	28.8	4.1	28.7	[26.5 – 31.3]
$\theta_{BSA \text{ on } V1}$	1.23	7.6	1.24	[1.07 – 1.47]
$V2 \text{ (L)} = \theta_{V2} \cdot (BSA/1.254)^{\theta_{BSA \text{ on } V2}}$				
$\theta_{V2}$	33.8	5.2	33.8	[30.7 – 37.2]
$\theta_{BSA \text{ on } V2}$	0.883	11.1	0.882	[0.671 – 1.06]

Parameter	Estimate	RSE (%)	Bootstrap median	Bootstrap 95% CI
<b>Q (L/h)</b>				
$\theta_Q$	5.81	8.1	5.84	[5.03 – 6.89]
<b>Inter-individual variability</b>				
CL (%CV)	26.3	11.4	25.1	[18.8 – 31.7]
V1 (%CV)	23.9	11.8	23.3	[16.9 – 28.5]
V2 (%CV)	25.9	18.2	24.9	[14.4 – 33.5]
Q (%CV)	35.1	20.0	33.9	[15.7 – 49.6]
Correlation between CL and V1	0.0492	21.7	0.0463	[0.028 – 0.0692]
Correlation between CL and V2	0.0341	34.6	0.0315	[0.0106 – 0.0573]

Parameter	Estimate	RSE (%)	Bootstrap median	Bootstrap 95% CI
Correlation between V1 and V2	0.0425	29.9	0.0398	[0.0165 – 0.0657]
<b>Residual variability</b>				
Proportional error (% CV)	17.5	4.7	17.5	[15.9 – 19.2]

RSE: relative standard error, CI: confidence interval, CL: clearance, BSA: body surface area, V1: central volume of distribution, V2: peripheral volume of distribution, Q: inter-compartmental clearance, CV: coefficient of variation.

The goodness-of-fit plots of the final model indicated good agreement between the observed and predicted F-ara-A plasma concentrations without an apparent trend in the residuals (Figure 1). The visual predictive checks showed that the 5<sup>th</sup>, 50<sup>th</sup> and 95<sup>th</sup> percentiles of the observed concentrations were within the 95% CIs around the predicted 5<sup>th</sup>, 50<sup>th</sup> and 95<sup>th</sup> percentiles of the simulated data using the final model (Figure 2). In addition, the parameters estimated from the final model were close to the median values determined from bootstrapping with 1,000 replicates, indicating a robust model with good precision (Table 3).

The PK profile were similar to the previously published data from the population aged between 12.6 and 65.5 years. The most of the observed concentrations were within the range between 5<sup>th</sup> and 95<sup>th</sup> percentile of predicted concentration (Figure 3).

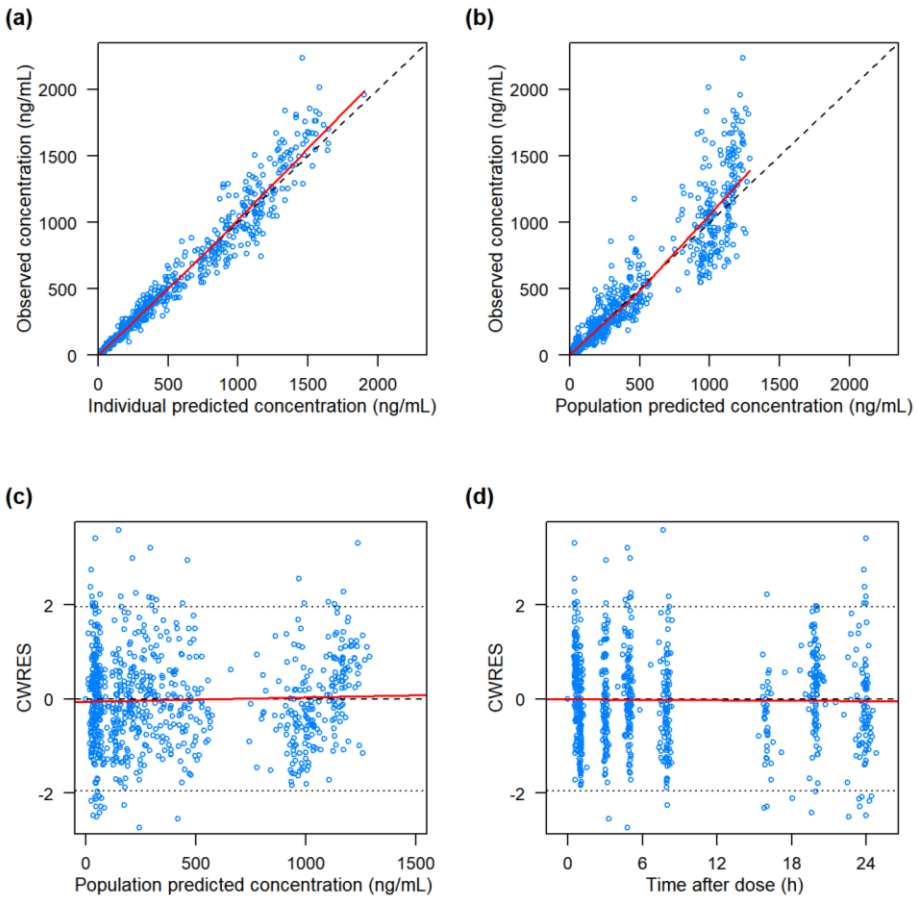


**Figure 1.** Goodness-of-fit plots for the plasma  $9-\beta$ -D-arabinofuranosyl-2-fluoroadenine (F-ara-A) concentration.

(a) Individual predictions versus observed concentrations, (b) population predictions versus observed concentrations, (c) conditional weighted residuals (CWRES) versus population predictions, (d) CWRES versus time after dose. Dashed lines represent the lines of identity (upper) or null values (lower), and solid lines reflect loess smoothing of the data.

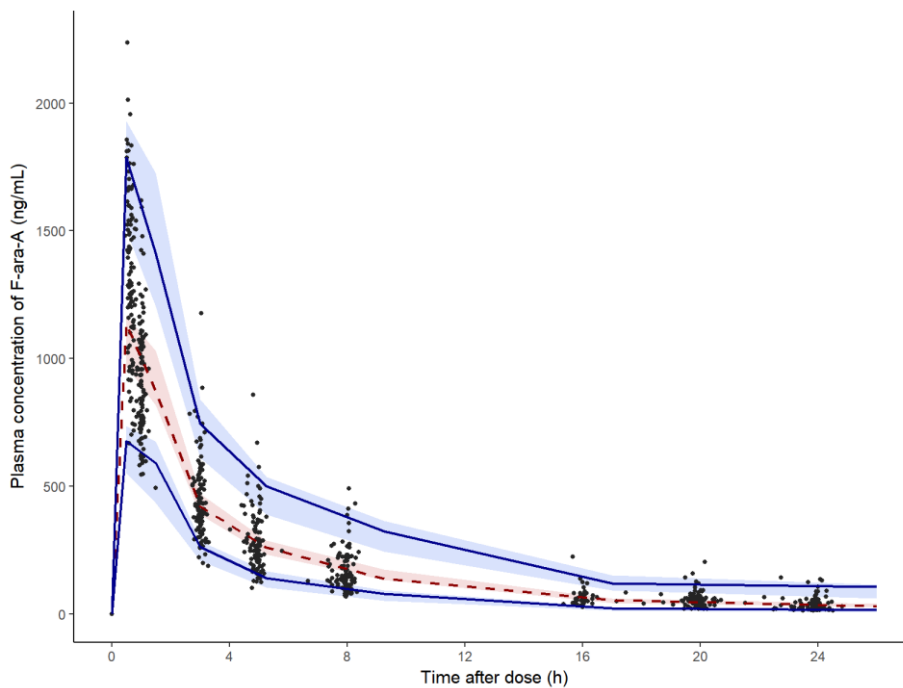


**Figure 2.** Visual predictive check of the plasma concentration–time profiles of 9– $\beta$ –D–arabinofuranosyl–2–fluoroadenine (F–ara–A) using the final model.

The dots are the individual observations, the dashed line is the 50<sup>th</sup> percentile and the solid lines are the 5<sup>th</sup> and 95<sup>th</sup> percentiles of the observed data. The shaded areas are the 95% confidence intervals around the predicted 5<sup>th</sup>, 50<sup>th</sup> and 95<sup>th</sup> percentiles of the simulated data.

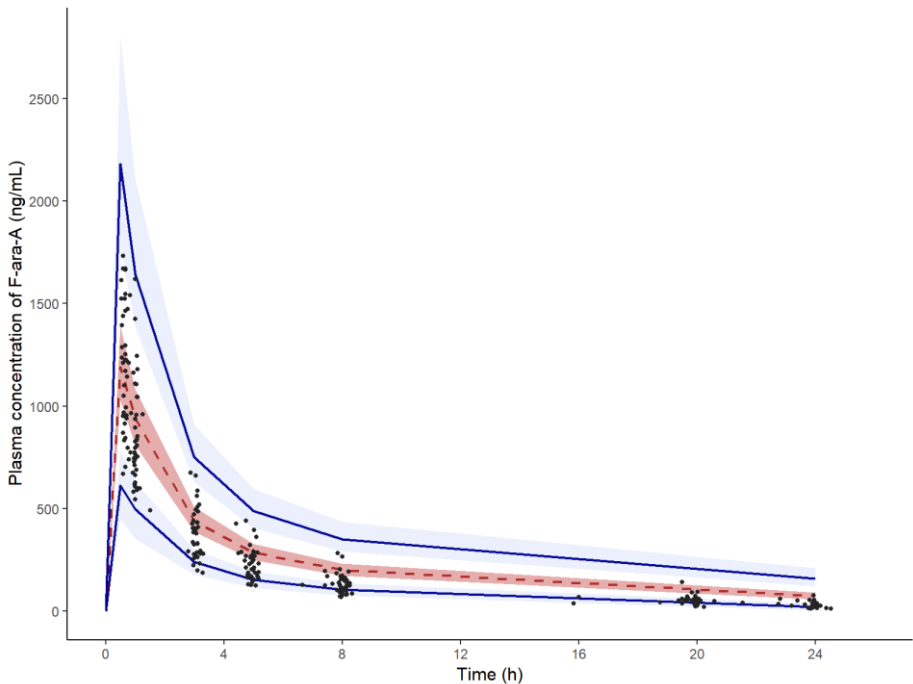


**Figure 3.** Visual predictive check comparing the observed plasma concentration–time profiles of 9– $\beta$ –D–arabinofuranosyl–2–fluoroadenine (F–ara–A) to the simulated data from previously published pharmacokinetic model (30).

The dots are the individual observations, the dashed line is the 50<sup>th</sup> percentile and the solid lines are the 5<sup>th</sup> and 95<sup>th</sup> percentiles of the simulated data. The shaded areas are the 95% confidence intervals around the predicted 5<sup>th</sup>, 50<sup>th</sup> and 95<sup>th</sup> percentiles of the simulated data. The observed and simulated data shows concentrations after the first dose of fludarabine at 40 mg/m<sup>2</sup>.

The AUC<sub>cum</sub> of F-ara-A during 5 or 6 days of fludarabine administration ranged from 17,185 to 60,741 ng·h/mL, with a median value of 27,133 ng·h/mL (Figure 4). Three patients who received a five-day regimen had AUC<sub>cum</sub> values between 17,185 and 26,015 ng·h/mL. The PK parameters of F-ara-A after the first dose of fludarabine at 40 mg/m<sup>2</sup> were calculated for 41 patients (Figure 5, Table 4). The C<sub>max</sub>, AUC<sub>0-24</sub>, and AUC<sub>inf</sub> of 37 patients whose fludarabine dose remained at 40 mg/m<sup>2</sup> for 6 days were 1,180 ng/mL, 4,707 ng·h/mL, and 5,220 ng·h/mL, respectively, after the sixth dose. The mean accumulation ratio was 1.09 for the 37 patients with mean AUC<sub>0-24</sub> values of 4,423 and 4,829 ng·h/mL for the first and sixth doses, respectively.

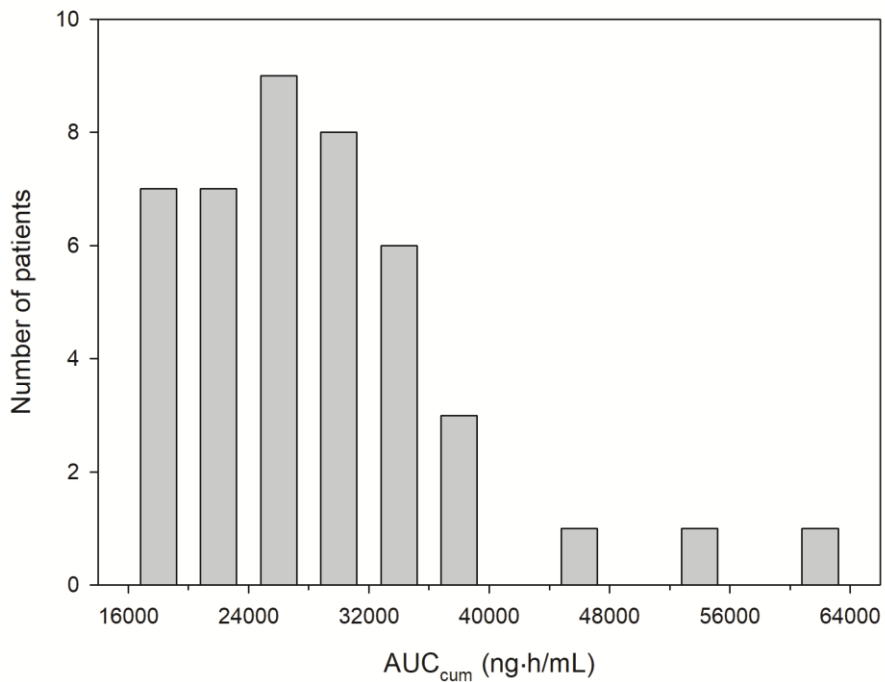


Figure 4. Number of patients according to the cumulative area under the concentration-time curve (AUC<sub>cum</sub>) of 9- $\beta$ -D-arabinofuranosyl-2-fluoroadenine (F-ara-A).

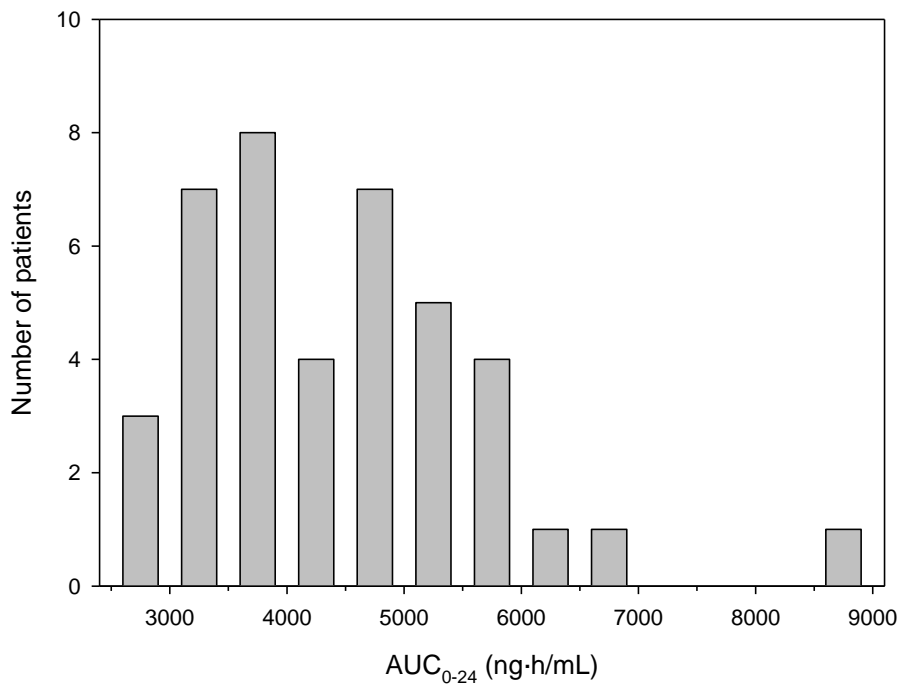


Figure 5. Number of patients according to the area under the concentration-time curve from dosing to 24 h post-dosing ( $\text{AUC}_{0-24}$ ) of 9- $\beta$ -D-arabinofuranosyl-2-fluoroadenine (F-ara-A) after the first dose of  $40 \text{ mg/m}^2$ .

Table 4. Pharmacokinetic parameters of 9- $\beta$ -D-arabinofuranosyl-2-fluoroadenine (F-ara-A) after the first dose of fludarabine at 40 mg/m<sup>2</sup>.

	Age < 5 (n = 5)	5 ≤ Age < 10 (n = 9)	10 ≤ Age < 15 (n = 18)	15 ≤ Age (n = 9)	Total (n = 41)
C <sub>max</sub> (ng/mL)	1,161 (1,102 – 1,509)	1,242 (756 – 1,490)	1,107 (852 – 1,700)	1,083 (761 – 1,534)	1,154 (756 – 1,700)
AUC <sub>0-24</sub> (ng·h/mL)	3,344 (2,916 – 4,816)	4,346 (2,900 – 5,360)	4,167 (2,977 – 8,746)	5,011 (3,159 – 5,863)	4,272 (2,900 – 8,746)
AUC <sub>inf</sub> (ng·h/mL)	3,443 (3,056 – 5,122)	4,569 (3,145 – 5,857)	4,602 (3,140 – 10,477)	5,695 (3,338 – 6,816)	4,696 (3,056 – 10,477)
t <sub>1/2</sub> (h)	6.91 (5.49 – 7.27)	7.77 (5.81 – 9.28)	8.22 (5.76 – 10.88)	9.39 (4.78 – 10.60)	7.95 (4.78 – 10.88)

The data are presented as the median (min – max).

$C_{\max}$ , maximum concentration;  $AUC_{0-24}$ , area under the concentration–time curve from dosing to 24 h post–dosing;  
 $AUC_{\text{inf}}$ , AUC from dosing to infinity;  $t_{1/2}$ , terminal elimination half–life.

## Exposure–clinical outcome relationships

A total of 43 patients were included in the exploratory analysis of the relationships between systemic fludarabine exposure and various clinical outcomes, including complications, GVHD, relapse and survival. No significant differences were found in the  $AUC_{cum}$  according to any individual clinical outcome variable (Figure 6). In addition, the incidences for all of the toxicities were not significantly different regardless of whether the cumulative exposure exceeded the median value of 27,133 ng·h/mL (Table 5). The cumulative incidences of aGVHD, cGVHD and relapse were not different between the patients with high and low  $AUC_{cum}$  values when the median value was used as a cut-off point ( $P = 0.569$ ,  $0.390$  and  $0.830$ , respectively). The OS and EFS rates were also not different between the 2 groups ( $P = 0.259$  and  $P = 0.342$ , respectively, Figure 7). Similarly,  $C_{max}$  during the treatment period was not associated with any of the clinical outcome variables (Figure 8).

When 6 subjects with an  $AUC_{cum}$  above 36,000 ng·h/mL were grouped as the high-exposure group for further analysis,

the rate of veno-occlusive disease (VOD), non-infectious pulmonary complications and neurologic complications were higher in the high-exposure group without reaching statistical significance (Table 6). The OS and EFS rates were not different in the high-exposure group compared with the other patients ( $P = 0.400$  and  $P = 0.612$ , respectively, Figure 9).

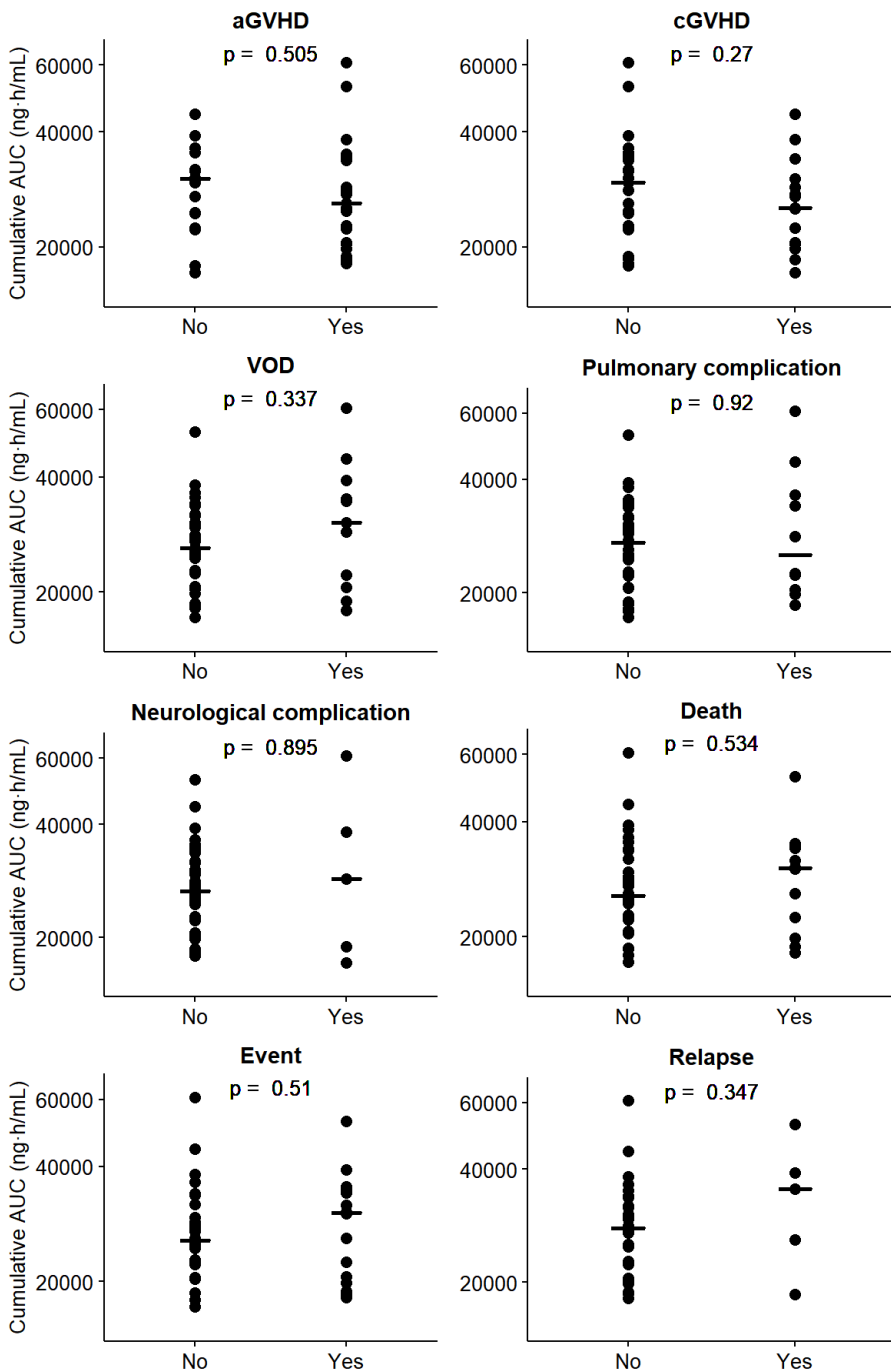


**Figure 6.** Relationships between the cumulative area under the curve (AUC) of 9- $\beta$ -D-arabinofuranosyl-2-fluoroadenine (F-ara-A) and the clinical outcomes.

The line represents the median value. The Mann-Whitney U test was used for the analysis. The Y-axes are presented on a logarithmic scale. All variables included 43 subjects in the analysis except for relapse, which included 31 subjects with malignant disease.

aGVHD, acute graft-versus-host disease; cGVHD, chronic graft-versus-host-disease; VOD, veno-occlusive disease

Table 5. Incidence of complications after fludarabine administration according to 9- $\beta$ -D-arabinofuranosyl-2-fluoroadenine (F-ara-A) exposure using median value as a cut-off.

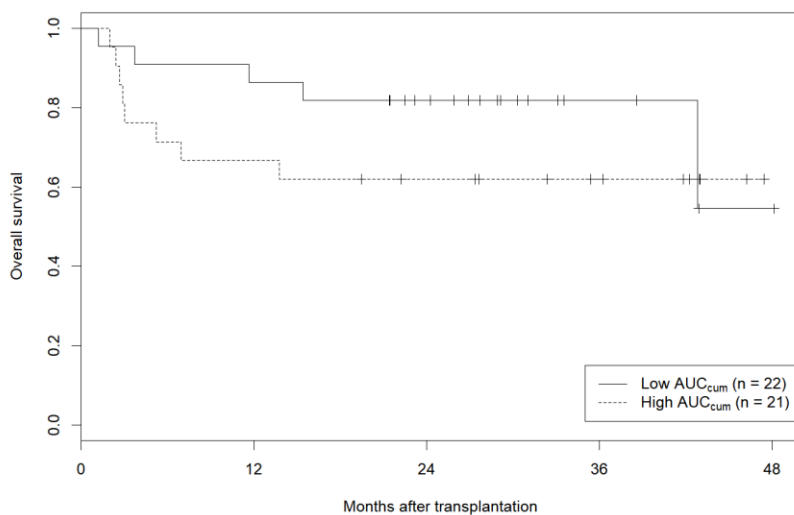
	Low AUC <sub>cum</sub> (n = 22)	High AUC <sub>cum</sub> (n = 21)	P – value <sup>a</sup>
Veno-occlusive disease	18.2% (4)	33.3% (7)	0.310
Non-infectious pulmonary complications ( $\geq$ grade 3)	22.7% (5)	23.8% (5)	1.00
Neurological complications ( $\geq$ grade 2)	9.1% (2)	14.3% (3)	0.664

The data are presented as the percent (number of subjects).

<sup>a</sup> Fisher's exact test.

AUC<sub>cum</sub>, cumulative area under the concentration-time curve.

(a)



(b)

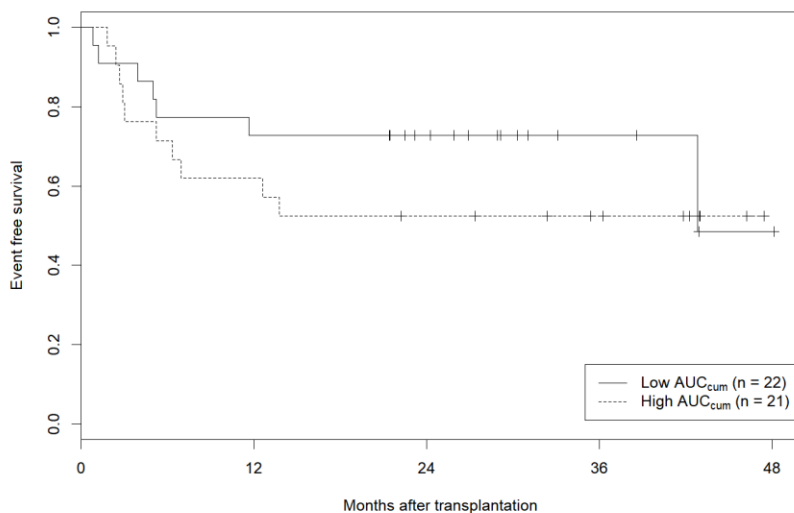
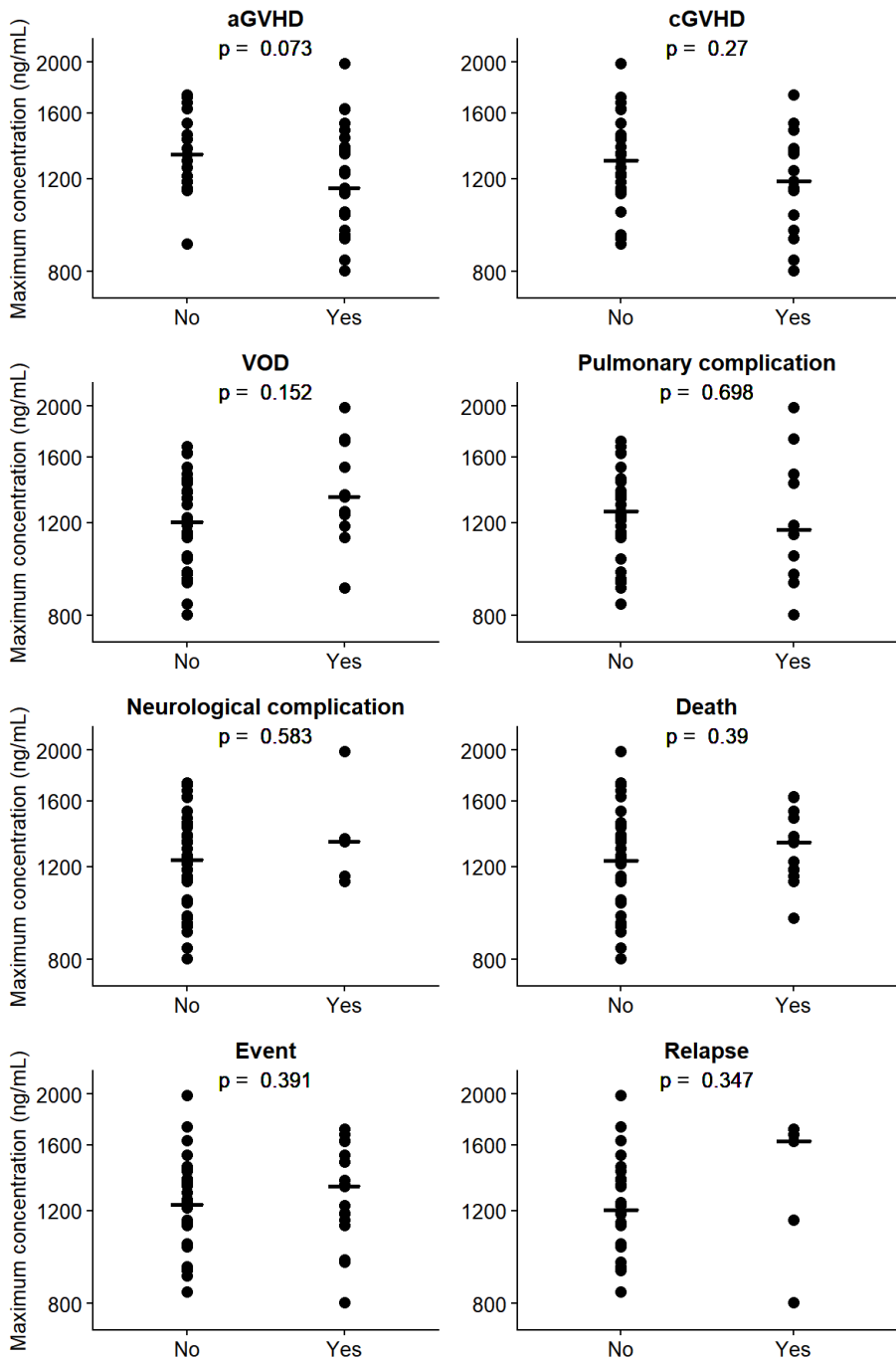


Figure 7. (a) Overall survival and (b) event-free survival according to cumulative area under the concentration-time curve ( $AUC_{cum}$ ) of 9- $\beta$ -D-arabinofuranosyl-2-fluoroadenine (F-ara-A) using median value as a cut-off.



**Figure 8. Relationships between the maximum concentration of 9- $\beta$ -D-arabinofuranosyl-2-fluoroadenine (F-ara-A) and the clinical outcomes.**

The line represents the median value. The Mann-Whitney U test was used for the analysis. The Y-axes are presented on a logarithmic scale. All variables included 43 subjects in the analysis except for relapse, which included 31 subjects with malignant disease.

aGVHD, acute graft-versus-host disease; cGVHD, chronic graft-versus-host-disease; VOD, veno-occlusive disease

Table 6. Incidence of complications after fludarabine administration according to 9- $\beta$ -D-arabinofuranosyl-2-fluoroadenine (F-ara-A) exposure using 36,000 ng·h/mL as a cut-off.

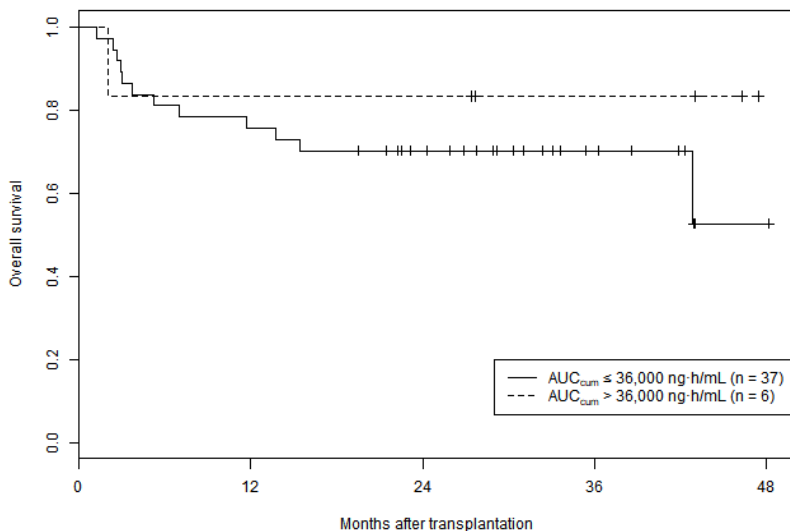
	Low AUC <sub>cum</sub> (n = 37)	High AUC <sub>cum</sub> (n = 6)	P – value <sup>a</sup>
Veno-occlusive disease	21.6% (8)	50.0% (3)	0.164
Non-infectious pulmonary complications ( $\geq$ grade 3)	18.9% (7)	50.0% (3)	0.127
Neurological complications ( $\geq$ grade 2)	8.1% (3)	33.3% (2)	0.135

Data are presented as the percent (number of subjects).

<sup>a</sup> Fisher's exact test.

AUC<sub>cum</sub>, cumulative area under the concentration-time curve.

(a)



(b)

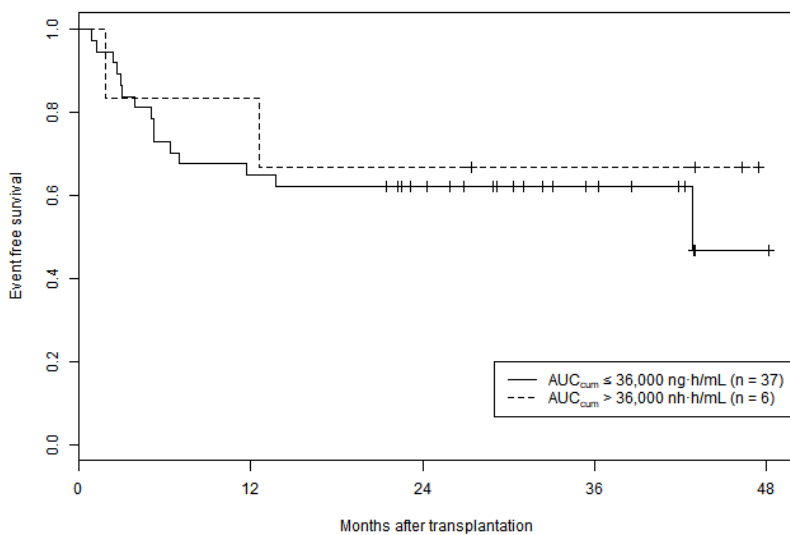


Figure 9. (a) Overall survival and (b) event-free survival according to cumulative area under the concentration-time curve ( $AUC_{cum}$ ) of 9- $\beta$ -D-arabinofuranosyl-2-fluoroadenine (F-ara-A) using 36,000 ng·h/mL as a cut-off.

## DISCUSSION

Despite the widespread use of fludarabine in conditioning regimens for HSCT, knowledge regarding the PK characteristics of fludarabine administered once daily in paediatric patients is limited. This study provides PK data in paediatric HSCT patients with additional exploration of its associations with clinical outcomes. The population PK analysis enabled exploration of the cumulative exposure during treatment despite the limited sampling time points and variable dosing regimens among the patients (31).

PK profile of fludarabine in paediatric patients was comparable to previous reports. The predicted profile based on PK model built from population with median (range) age of 51.9 (12.6 – 65.5) years were similar to our observed data in children (30). Furthermore, the  $AUC_{inf}$  and  $t_{1/2}$  of paediatric patients were similar to those reported in another study with adults (16). When fludarabine was administered at  $40 \text{ mg/m}^2$ , the median  $AUC_{inf}$  and  $t_{1/2}$  values were  $4.7 \text{ mg}\cdot\text{h/L}$  and  $7.95 \text{ h}$  in the paediatric patients and  $4.9 \text{ mg}\cdot\text{h/L}$  and  $8.53 \text{ h}$  in the adult patients, respectively. The

minimum and maximum  $AUC_{inf}$  values in the paediatric patients were within the range of those reported in adults, indicating that paediatric patients were unlikely to show higher variability compared to adults (16). The PK parameters were comparable among the age groups in our study, while patients aged less than 5 years showed a tendency of lower exposure. A higher GFR with a median value of  $175.3 \text{ mL/min}/1.73 \text{ m}^2$  likely contributed to the lower exposure of these 5 patients compared to the others. The exposure found in this study, which was evaluated in Korean patients, was also comparable to that reported in a recent paediatric study conducted in the US (22), suggesting no effect of ethnicity on fludarabine pharmacokinetics. Similarly, a previous phase 1 study of oral fludarabine phosphate in Japanese reported comparable PK results to those obtained from Caucasians (32).

F-ara-A is largely eliminated by renal excretion, and decreased clearance in patients with renal impairment has been reported previously (17, 33, 34). Even after the dosage of fludarabine was reduced to  $30 \text{ mg}/\text{m}^2/\text{day}$  for 1 patient whose GFR was  $60.9 \text{ mL/min}/1.73 \text{ m}^2$ , the patient had a higher  $AUC_{cum}$

(52,604 ng·h/mL) than most of the patients. Accordingly, GFR was a covariate for CL in our PK model. Nevertheless, most of the patients had normal functions, and all patients enrolled in the study had adequate renal functions ( $> 60$  mL/min/1.73 m<sup>2</sup>). Therefore, the PK parameters may differ in patients with renal impairment, and caution is necessary when applying the model to those patients.

Other agents used for the conditioning regimen likely did not affect the pharmacokinetics of fludarabine observed in our study. Among 43 patients, 41 patients received busulfan with fludarabine and 2 patients with severe aplastic anaemia received cyclophosphamide before starting fludarabine. Previous study reported no changes in the PK parameters of fludarabine given before and after busulfan, implying the absence of a drug–drug interaction (35). Although no information on the PK interaction between cyclophosphamide and fludarabine is available, no evidence supports a change in fludarabine exposure due to cyclophosphamide administration considering that renal excretion is the major route of elimination of fludarabine. The 2 patients who received cyclophosphamide had AUC<sub>inf</sub> values of

5,261 and 3,454 ng·h/mL, which are comparable to the values of other patients. Other agents, including etoposide and melphalan, were started when fludarabine administration was about to end, limiting the possibility that they affected fludarabine pharmacokinetics.

Despite the extensive need for paediatric clinical trials to ensure safe and effective drug use, the number of subjects enrolled in the trials should be minimized due to ethical concerns and the vulnerability of this population. This limitation increases the need to maximize the use of adult data and extrapolate these data to the paediatric population (36). Generally, when no separate efficacy studies have been conducted, PK studies should be used to determine how to adjust the dosage regimen to achieve the same level of systemic exposure reported in adults in paediatric dose selection (37). Comparable exposure in adults shown in our study may support the appropriateness of BSA-based dosing.

Although not statistically significant, the incidence of complications tended to be higher in patients with high F-ara-A

exposure than the others when AUC<sub>cum</sub> of 36,000 ng·h/mL was used as a cut-off. Pulmonary and neurotoxicity induced by fludarabine has been previously reported (38–41), and our findings suggest that these complications might be associated with the degree of systemic fludarabine exposure, which could be preventable. Nevertheless, confirming the associations between exposure and clinical outcomes is difficult because the subjects in our study had a wide range of ages as well as various indications with different conditioning regimens, which could have confounded the associations.

No associations were found between exposure and relapse, survival or GVHD, which is with the result from the only available PK study of fludarabine in paediatric HSCT patients, where no association between F-ara-A exposure and TRM was found (22). However, the results were not in line with the previously reported association between a high F-ara-A exposure and an increased risk of TRM or between a low clearance and an increased risk of aGVHD in adults (16, 17). It is possible that the limited number of patients in this study had insufficient power for detecting these associations. Moreover, the large inter-

individual variability of up to 39-fold in intracellular F-ara-ATP accumulation suggests complex relationships between systemic F-ara-A exposure and clinical outcomes (21, 42). One study revealed an association between fludarabine toxicity and a genetic polymorphism in deoxycytidine kinase, which metabolizes fludarabine (43). Such pharmacogenetic approaches may improve our understanding of the variability of clinical outcomes and their associations with pharmacokinetics.

In conclusion, this study evaluated the pharmacokinetics of F-ara-A after fludarabine administration in paediatric HSCT patients. The results were comparable to those found in previous studies with different populations. This approach provides evidence for the safer use of fludarabine in paediatric patients, which has previously been empirically administered.

## REFERENCES

1. Batchelor HK, Marriott JF. Paediatric pharmacokinetics: key considerations. *British journal of clinical pharmacology*. 2015;79(3):395–404.
2. Bornhauser M, Storer B, Slattery JT, Appelbaum FR, Deeg HJ, Hansen J, et al. Conditioning with fludarabine and targeted busulfan for transplantation of allogeneic hematopoietic stem cells. *Blood*. 2003;102(3):820–6.
3. Andersson BS, de Lima M, Thall PF, Wang X, Couriel D, Korbling M, et al. Once daily i.v. busulfan and fludarabine (i.v. Bu-Flu) compares favorably with i.v. busulfan and cyclophosphamide (i.v. BuCy2) as pretransplant conditioning therapy in AML/MDS. *Biol Blood Marrow Transplant*. 2008;14(6):672–84.
4. Chae YS, Sohn SK, Kim JG, Cho YY, Moon JH, Shin HJ, et al. New myeloablative conditioning regimen with fludarabine and busulfan for allogeneic stem cell transplantation: comparison with BuCy2. *Bone Marrow Transplant*. 2007;40(6):541–7.
5. Chaudhry M, Ali N. Reduced-intensity conditioning hematopoietic stem cell transplantation: looking forward to an

- international consensus. *Blood research*. 2015;50(2):69–70.
6. Lei XR, Chen HL, Wang FX, Bai J, He AL. Busulfan plus fludarabine compared with busulfan plus cyclophosphamide as a conditioning regimen prior to hematopoietic stem cell transplantation in patients with hematologic neoplasms: a meta-analysis. *International journal of clinical and experimental medicine*. 2015;8(8):12064–75.
7. Label: Fludarabine Phosphate Injection 2010 [updated Dec 2010; cited 2017 29 June]. Available from: [https://www.accessdata.fda.gov/drugsatfda\\_docs/label/2011/022137s003lbl.pdf](https://www.accessdata.fda.gov/drugsatfda_docs/label/2011/022137s003lbl.pdf).
8. Bartelink IH, van Reij EM, Gerhardt CE, van Maarseveen EM, de Wildt A, Versluys B, et al. Fludarabine and exposure-targeted busulfan compares favorably with busulfan/cyclophosphamide-based regimens in pediatric hematopoietic cell transplantation: maintaining efficacy with less toxicity. *Biol Blood Marrow Transplant*. 2014;20(3):345–53.
9. Ishida H, Adachi S, Hasegawa D, Okamoto Y, Goto H, Inagaki J, et al. Comparison of a fludarabine and melphalan combination-based reduced toxicity conditioning with

myeloablative conditioning by radiation and/or busulfan in acute myeloid leukemia in Japanese children and adolescents. *Pediatr Blood Cancer*. 2015;62(5):883–9.

10. Güngör T, Teira P, Slatter M, Stussi G, Stepensky P, Moshous D, et al. Reduced-intensity conditioning and HLA-matched haemopoietic stem-cell transplantation in patients with chronic granulomatous disease: a prospective multicentre study. *The Lancet*. 2014;383(9915):436–48.

11. Seo JJ. Hematopoietic cell transplantation for hemophagocytic lymphohistiocytosis: recent advances and controversies. *Blood research*. 2015;50(3):131–9.

12. Gandhi V, Plunkett W. Cellular and clinical pharmacology of fludarabine. *Clinical pharmacokinetics*. 2002;41(2):93–103.

13. Huang P, Chubb S, Plunkett W. Termination of DNA synthesis by 9-beta-D-arabinofuranosyl-2-fluoroadenine. A mechanism for cytotoxicity. *The Journal of biological chemistry*. 1990;265(27):16617–25.

14. Danhauser L, Plunkett W, Keating M, Cabanillas F. 9-beta-D-arabinofuranosyl-2-fluoroadenine 5'-monophosphate pharmacokinetics in plasma and tumor cells of patients with

relapsed leukemia and lymphoma. *Cancer Chemother Pharmacol.* 1986;18(2):145–52.

15. Gandhi V, Kemen A, Keating MJ, Plunkett W. Cellular pharmacology of fludarabine triphosphate in chronic lymphocytic leukemia cells during fludarabine therapy. *Leukemia & lymphoma.* 1993;10(1–2):49–56.

16. Long-Boyle JR, Green KG, Brunstein CG, Cao Q, Rogoscheske J, Weisdorf DJ, et al. High fludarabine exposure and relationship with treatment-related mortality after nonmyeloablative hematopoietic cell transplantation. *Bone Marrow Transplant.* 2011;46(1):20–6.

17. Sanghavi K, Wiseman A, Kirstein MN, Cao Q, Brundage R, Jensen K, et al. Personalized fludarabine dosing to reduce nonrelapse mortality in hematopoietic stem-cell transplant recipients receiving reduced intensity conditioning. *Translational research : the journal of laboratory and clinical medicine.* 2016;175:103–15 e4.

18. Griffiths CD, Ng ES, Kangaloo SB, Williamson TS, Chaudhry MA, Booker R, et al. Fludarabine metabolite level on day zero does not affect outcomes of hematopoietic cell

- transplantation in patients with normal renal function. *Bone Marrow Transplant.* 2014;49(4):589–91.
19. Mohanan E, Panetta JC, Lakshmi KM, Edison ES, Korula A, Fouzia NA, et al. Population pharmacokinetics of fludarabine in patients with aplastic anemia and Fanconi anemia undergoing allogeneic hematopoietic stem cell transplantation. *Bone Marrow Transplant.* 2017;52(7):977–83.
20. McCune JS, Woodahl EL, Furlong T, Storer B, Wang J, Heimfeld S, et al. A pilot pharmacologic biomarker study of busulfan and fludarabine in hematopoietic cell transplant recipients. *Cancer Chemother Pharmacol.* 2012;69(1):263–72.
21. McCune JS, Mager DE, Bemer MJ, Sandmaier BM, Storer BE, Heimfeld S. Association of fludarabine pharmacokinetic/dynamic biomarkers with donor chimerism in nonmyeloablative HCT recipients. *Cancer Chemother Pharmacol.* 2015;76(1):85–96.
22. Ivaturi V, Dvorak CC, Chan D, Liu T, Cowan MJ, Wahlstrom J, et al. Pharmacokinetics and Model-Based Dosing to Optimize Fludarabine Therapy in Pediatric Hematopoietic Cell Transplant Recipients. *Biol Blood Marrow Transplant.*

2017;23(10):1701–13.

23. McCune JS, Jacobson P, Wiseman A, Militano O. Optimizing drug therapy in pediatric SCT: focus on pharmacokinetics. *Bone Marrow Transplant*. 2015;50(2):165–72.
24. Avramis VI, Wiersma S, Kralio MD, Ramilo-Torno LV, Sharpe A, Liu-Mares W, et al. Pharmacokinetic and pharmacodynamic studies of fludarabine and cytosine arabinoside administered as loading boluses followed by continuous infusions after a phase I/II study in pediatric patients with relapsed leukemias. The Children's Cancer Group. *Clin Cancer Res*. 1998;4(1):45–52.
25. Avramis VI, Champagne J, Sato J, Kralio M, Ettinger LJ, Poplack DG, et al. Pharmacology of fludarabine phosphate after a phase I/II trial by a loading bolus and continuous infusion in pediatric patients. *Cancer research*. 1990;50(22):7226–31.
26. Lee JW, Kang HJ, Lee SH, Yu KS, Kim NH, Yuk YJ, et al. Highly variable pharmacokinetics of once-daily intravenous busulfan when combined with fludarabine in pediatric patients: phase I clinical study for determination of optimal once-daily

busulfan dose using pharmacokinetic modeling. *Biol Blood Marrow Transplant.* 2012;18(6):944–50.

27. Lee JW, Kang HJ, Kim S, Lee SH, Yu KS, Kim NH, et al. Favorable outcome of hematopoietic stem cell transplantation using a targeted once-daily intravenous busulfan–fludarabine–etoposide regimen in pediatric and infant acute lymphoblastic leukemia patients. *Biol Blood Marrow Transplant.* 2015;21(1):190–5.

28. Mortensen JB, Rodbro P. Comparison between total and renal plasma clearance of [51Cr] EDTA. *Scandinavian journal of clinical and laboratory investigation.* 1976;36(3):247–9.

29. Fleming JS, Zivanovic MA, Blake GM, Burniston M, Cosgriff PS, British Nuclear Medicine S. Guidelines for the measurement of glomerular filtration rate using plasma sampling. *Nuclear medicine communications.* 2004;25(8):759–69.

30. Salinger DH, Blough DK, Vicini P, Anasetti C, O'Donnell PV, Sandmaier BM, et al. A limited sampling schedule to estimate individual pharmacokinetic parameters of fludarabine in hematopoietic cell transplant patients. *Clin Cancer Res.* 2009;15(16):5280–7.

31. Sheiner LB, Rosenberg B, Marathe VV. Estimation of population characteristics of pharmacokinetic parameters from routine clinical data. *Journal of pharmacokinetics and biopharmaceutics*. 1977;5(5):445–79.
32. Ogawa Y, Hotta T, Tobinai K, Watanabe T, Sasaki Y, Minami H, et al. Phase I and pharmacokinetic study of oral fludarabine phosphate in relapsed indolent B-cell non-Hodgkin's lymphoma. *Annals of oncology : official journal of the European Society for Medical Oncology*. 2006;17(2):330–3.
33. Lichtman SM, Etcubanas E, Budman DR, Eisenberg P, Zervos G, D'Amico P, et al. The pharmacokinetics and pharmacodynamics of fludarabine phosphate in patients with renal impairment: a prospective dose adjustment study. *Cancer investigation*. 2002;20(7–8):904–13.
34. Kemeny A, Fernandez M, Bauman J, Keating M, Plunkett W. A sensitive fluorescence assay for quantitation of fludarabine and metabolites in biological fluids. *Clinica chimica acta; international journal of clinical chemistry*. 1991;200(2–3):95–106.
35. Bonin M, Pursche S, Bergeman T, Leopold T, Illmer T,

Ehninger G, et al. F-ara-A pharmacokinetics during reduced-intensity conditioning therapy with fludarabine and busulfan.

Bone Marrow Transplant. 2007;39(4):201–6.

36. Dunne J, Rodriguez WJ, Murphy MD, Beasley BN, Burckart GJ, Filie JD, et al. Extrapolation of adult data and other data in pediatric drug-development programs. Pediatrics. 2011;128(5):e1242–9.

37. Draft Guidance for Industry: General Clinical Pharmacology Considerations for Pediatric Studies for Drugs and Biological Products: US Food and Drug Administration; [cited 2017 June 20]. Available from: <https://www.fda.gov/downloads/drugs/guidances/ucm425885.pdf>.

38. Helton KJ, Patay Z, Triplett BM. Fludarabine-induced severe necrotizing leukoencephalopathy in pediatric hematopoietic cell transplantation. Bone Marrow Transplant. 2013;48(5):729–31.

39. Cheson BD, Vena DA, Foss FM, Sorensen JM. Neurotoxicity of purine analogs: a review. Journal of clinical oncology : official journal of the American Society of Clinical

Oncology. 1994;12(10):2216–28.

40. Disel U, Paydas S, Yavuz S, Karakoc E. Severe pulmonary toxicity associated with fludarabine and possible contribution of rituximab. *Cancer Chemotherapy*. 2010;56(2):89–93.

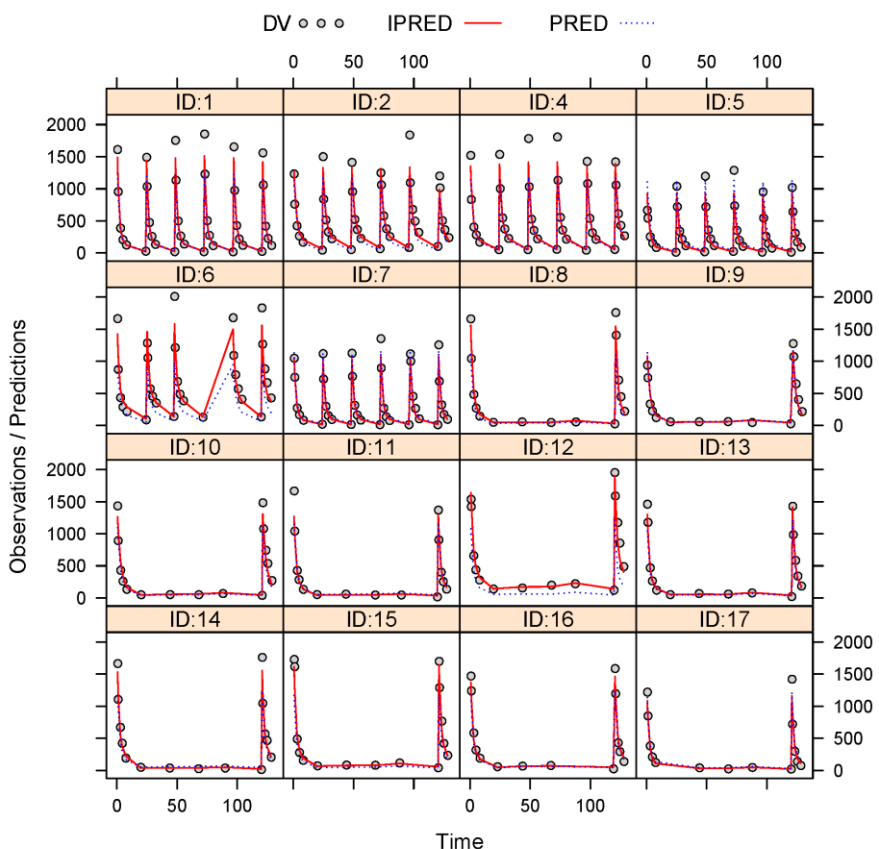
41. Helman DL, Jr., Byrd JC, Ales NC, Shorr AF. Fludarabine-related pulmonary toxicity: a distinct clinical entity in chronic lymphoproliferative syndromes. *Chest*. 2002;122(3):785–90.

42. Woodahl EL, Wang J, Heimfeld S, Sandmaier BM, O'Donnell PV, Phillips B, et al. A novel phenotypic method to determine fludarabine triphosphate accumulation in T-lymphocytes from hematopoietic cell transplantation patients. *Cancer Chemother Pharmacol*. 2009;63(3):391–401.

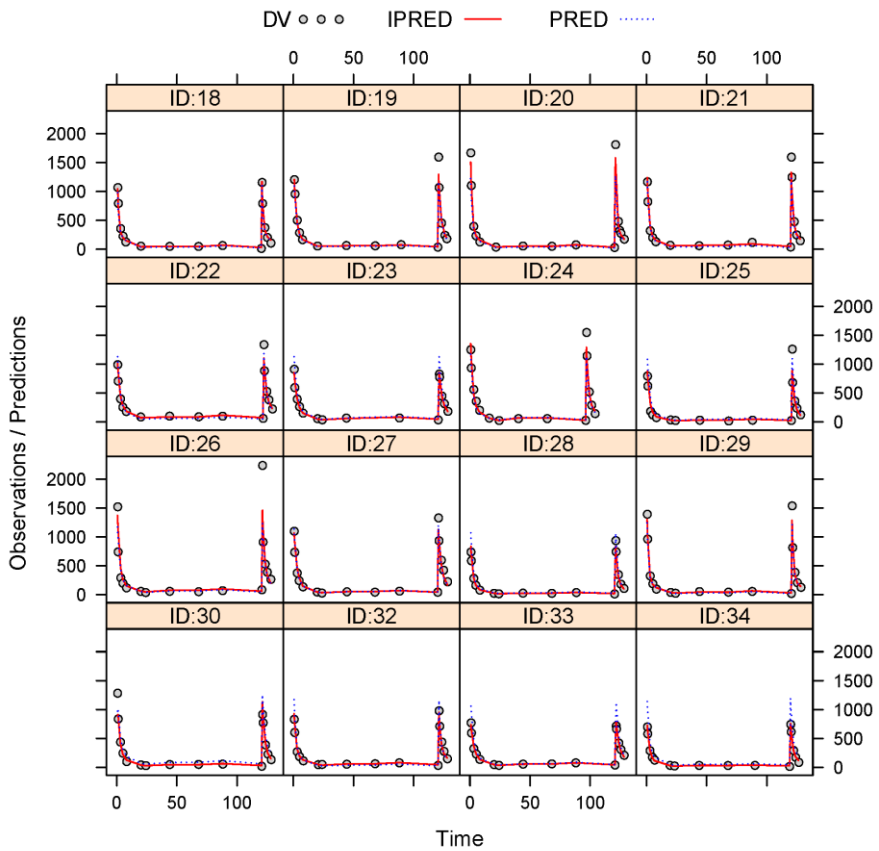
43. Rivero A, Rapado I, Tomas JF, Montalban C, de Ona R, Paz-Carreira J, et al. Relationship between deoxycytidine kinase (DCK) genotypic variants and fludarabine toxicity in patients with follicular lymphoma. *Leuk Res*. 2011;35(4):431–7.

# APPENDICES

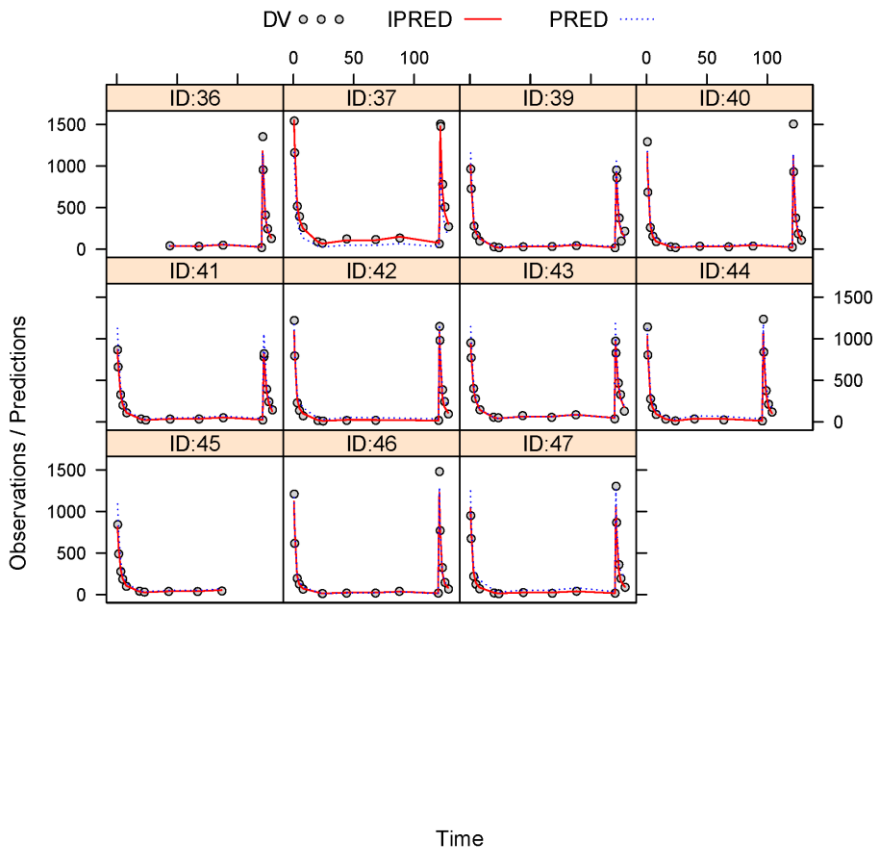
## 1. Individual fitting plots



## 1. Individual fitting plots (Continued)



## 1. Individual fitting plots (Continued)



## 2. NONMEM control for the final model

\$SUBROUTINES ADVAN3 TRANS4

\$PK

TVCL = THETA(1) \* (BSA/1.254)\*\*THETA(8) \*  
(nGFR/132.6)\*\*THETA(10)

TVV1 = THETA(2) \* (BSA/1.254)\*\*THETA(7)

TVV2 = THETA(3) \* (BSA/1.254)\*\*THETA(9)

TVQ = THETA(4)

CL = TVCL\* EXP(ETA(1))

V1 = TVV1 \* EXP(ETA(2))

V2 = TVV2 \* EXP(ETA(3))

Q = TVQ \* EXP(ETA(4))

K = CL/V1

K12 = Q/V1

K21 = Q/V2

S1 = V1/1000

\$ERROR

IPRED = F

IRES = DV - IPRED

```
W = SQRT(THETA(5)**2+THETA(6)**2* IPRED**2)
IWRES = IRES/W
Y = F + W*EPS(1)
```

```
$THETA
(0, 10.8) ; CL
(0, 38.6) ; V1
(0, 44.6) ; V2
(0, 7.51) ; Q
(0.001) FIX ; additive error
(0.175) ; proportional error
(0, 1.22) ; V1~BSA POWER
(0, 0.824) ; CL~BSA POWER
(0, 0.874) ; V2~BSA POWER
(1) ; CL~nGFR
```

```
$OMEGA BLOCK(3)
0.0719 ; CL
0.045 0.0519 ; V1
0.0373 0.0412 0.0663 ; V2
$OMEGA
0.3 ; Q
```

```
$SIGMA
```

1 FIX

\$COVARIANCE

\$EST SIG=3 MAX=9999 PRINT=5 METHOD=1 INTER  
NOABORT

\$TABLE ID TIME TAD AMT RATE DV MDV DAY IPRED IWRES  
IRES CWRES ONEHEADER NOPRINT FILE=sdtab001

\$TABLE ID CL V1 V2 Q ETA1 ETA2 ETA3 ETA4 ONEHEADER  
NOPRINT FILE=patab001

\$TABLE ID AGE WEIGHT HEIGHT BSA BMI Cr nGFR  
ONEHEADER NOPRINT FILE=cotab001

\$TABLE ID SEX ONEHEADER NOPRINT FILE=catab001

## 국문 초록

**서론:** 플루다라빈은 조혈모세포이식을 위한 전처치 요법에 사용되는 약물이나, 소아에서의 1일 1회 용법에서의 약동학 양상은 제한적으로 알려져 있다. 본 연구에서는 소아 환자에서 플루다라빈의 약동학을 연구하고 약동학과 임상 결과와의 연관성을 탐색하고자 하였다.

**방법:** 조혈모세포이식을 시행하고 플루다라빈을 투여 받은 43 명의 소아 환자로부터 얻어진 802 개의 농도 자료가 비선형 혼합 효과 모형을 이용한 집단 약동학 분석에 포함되었다. 모형으로부터 얻어진 개인의 전신 노출을 바탕으로 F-ara-A의 노출과 임상 결과 변수와의 연관성을 탐색하였다.

**결과:** F-ara-A의 시간에 따른 혈중 농도 양상은 이구획 모형과 비례 잔차 모형으로 적절하게 설명되었다. 체표면적과 사구체 여과율은 F-ara-A의 청소율에 유의한 공변량으로 확인되었다. 이식편대 속주병, 재발, 및 생존률과 전신 노출 간의 연관은 확인되지 않았다.

**결론:** 본 연구는 소아 환자에서 플루다라빈 투여 후 F-ara-A의 약동학을 평가하였다. 성인에서 보고된 것과 비슷한 전신 노출은 체 표면적 기반 용법이 적절함을 뒷받침할 수 있다.

---

**주요어:** 약동학, 모델링, 소아, 플루다라빈

**학번:** 2013-21790